—Technical Note —

COMPUTATION OF STRESS INTENSITY FACTORS USING WAVELET-BASED ELEMENT

J.-W. Xiang *

College of Mechanical & Electrical Engineering
Wenzhou University
Wenzhou, China

Department of Mechanical Engineering
University of Ottawa
Ottawa, Canada

M. Liang

Department of Mechanical Engineering
University of Ottawa
Ottawa, Canada

Y.-T. Zhong

College of Mechanical & Electrical Engineering
Wenzhou University
Wenzhou, China

ABSTRACT

A new approach for the analysis of stress intensity factors (SIFs) for cracked plane plate is proposed based on the wavelet finite element method using the scaling functions of B-spline wavelet on the interval (BSWI). The performance of the method is investigated through the comparison of the results with the available numerical examples in the literate. It is shown that the solution quality is much better than that of the traditional adaptive finite element method. Though the method is applied to plane structures in this paper, it can be extended to solving problems for other classes of structures.

Keywords: Plate, Stress intensity factors, B-spline wavelet, Wavelet-based element.

1. INTRODUCTION

Finding the close-form solution of stress intensity factors (SIFs) is mathematically challenging. Among the existing fracture mechanics methods, the finite-element method has gained popularity in the past several decades [1].

To calculate SIFs more efficiently, some new numerical analysis methods are proposed recently. For example, Long *et al*. proposed a sub-region mixed finite element method to calculate SIFs for some finite and infinite plates [2,3]. Chen *et al*. developed a multilayer hybrid-stress finite element model together with two types of composite multilayer elements to analyze the influence of various crack parameters (position, length, thickness and fiber orientation) on the estimation of SIFs of composite laminates [4]. Different boundary element methods were applied by a number of researchers (*e.g.*, Miyazaki *et al*. [5], Lu *et al*. [6], Lu and Cheng [7], Chao and Wikarta [8] and Chao and Lu [9]) to analyze two-dimensional crack problems including biomaterial interface crack problems, dynamic propagation problem concerning Mode I crack, Asymmetrical dynamic propagation problem concerning Mode III crack, layered structures, respectively. Giner *et al*. proposed an Extended Finite Element Method (X-FEM) for the numerical analysis of crack problems and implemented it in the finite element code Abaqus [10]. For the finite element analysis of crack problems, adaptive mesh is also an important technique to obtain more precise value of SIFs. Kpegba and Ottavy proposed a method by the combination of two independent classical meshes to improve finite element analysis precision [11]. Souiyah *et al*. develop a two-dimensional finite element method to solve SIFs using the natural triangular quarter point elements to replace the collapsed quadrilateral elements [12]. Yang developed a special crack tip displacement discontinuity element to solve SIFs [13]. Meshii and Watanabe developed a novel singular finite element to simulate cracked plates and analyze the solution errors [14]. Daimon and Okada calculated Stress intensity factors using enriched crack tip finite elements in several typical mechanical loads [15].

Wavelet analysis is a useful tool to deal with engineering data [16,17]. In recent years, wavelet finite element method is proposed to solve the Partial Differential Equations (PDEs) [18]. Xiang *et al*. employed the scaling functions of B-spline wavelet on the interval (BSWI) as interpolating functions to construct two-dimensional wavelet-based plate elements [19,20]. Zhang *et al*. proposed a multivariable spline-based wavelet finite element method to analyze structural mechanics problems [21,22]. Yang *et al*. extended the BSWI wavelet-based element to analyze the plate buckling problem [23]. The advantages of the wavelet-

* Corresponding author (jwxiang@wzu.edu.cn)

DOI : 10.1017/jmech.2016.2
Copyright © 2016 The Society of Theoretical and Applied Mechanics, R.O.C.
https://doi.org/10.1017/jmech.2016.2 Published online by Cambridge University Press

based element as acknowledged in literatures include high precision and good flexibility of finite element interpolating bases [24,25].

In the present work, we propose an effective wavelet based BSWI method to calculate SIFs. Two numerical examples of the center crack and the double edge crack problems are investigated. Though the method as presented here is oriented toward plane structures, the feasibility to extend the approach to other classes of structures is obvious.

2. WAVELET-BASED ELEMENT FORMULAS TO CALCULATE SIFS

One-dimensional multi-resolution analysis (MRA) of BSWI on the interval [0,1] is given by Chui and Quak [26]. In the present, for the usage of only scaling functions at level $j = 3$, we start the 4th order wavelet bases in scaling space V_{j+1} as

$$\boldsymbol{\Phi}_4 = [\boldsymbol{\Phi}_3, \boldsymbol{\Psi}_3] \tag{1}$$

where $\boldsymbol{\Phi}_3 = \left[\phi^3_{4,-3}(\xi) \;\; \phi^3_{4,-2}(\xi) \;\; \cdots \;\; \phi^3_{4,7}(\xi)\right]$ represents scaling functions in V_3 and $\boldsymbol{\Psi}_3$ the wavelet bases in wavelet space W_3, *i.e.* $\boldsymbol{\Psi}_3 = \left[\psi^3_{4,-3}(\xi) \;\; \psi^3_{4,-2}(\xi) \cdots \psi^3_{4,4}(\xi)\right]$. The specifics of scaling functions and wavelets are listed in [20].

To construct two-dimensional wavelet bases, tensor product of one-dimensional wavelets is a simply and commonly used method [27]. In the present, take $\boldsymbol{\Phi}_4 = [\boldsymbol{\Phi}_3, \boldsymbol{\Psi}_3]$ for example, the two-dimensional scaling and wavelet functions are

$$\begin{aligned}\boldsymbol{\Phi}_4 \otimes \boldsymbol{\Phi}_4 &= [\boldsymbol{\Phi}_3 \otimes \boldsymbol{\Phi}_3, \boldsymbol{\Phi}_3 \otimes \boldsymbol{\Psi}_3, \boldsymbol{\Psi}_3 \otimes \boldsymbol{\Phi}_3, \boldsymbol{\Psi}_3 \otimes \boldsymbol{\Psi}_3] \\ &= [\boldsymbol{\Phi}^1, \boldsymbol{\Psi}^2, \boldsymbol{\Psi}^3, \boldsymbol{\Psi}^4]\end{aligned} \tag{2}$$

where $\otimes$ is the kronecker symbol. Therefore, we can obtain four functions, namely, the scaling functions $\boldsymbol{\Phi}^1 = \boldsymbol{\Phi}_3 \otimes \boldsymbol{\Phi}_3$ and wavelets $\boldsymbol{\Psi}^1 = \boldsymbol{\Psi}_3 \otimes \boldsymbol{\Phi}_3$, $\boldsymbol{\Psi}^2 = \boldsymbol{\Phi}_3 \otimes \boldsymbol{\Psi}_3$ and $\boldsymbol{\Psi}^3 = \boldsymbol{\Psi}_3 \otimes \boldsymbol{\Psi}_3$. As shown in Refs. [20], we can use only one formula to obtain any level of $\boldsymbol{\Phi}_j$ ($j \geq 3$) from the given $\boldsymbol{\Phi}_0$. Therefore, in this study, only scaling functions are adopted as interpolating bases and the BSWI element is employed to solve SIFs.

As was well known, a plane elasticity problem involves plane stress and plane strain problems. Once the plane stress problem is solved the plane strain problem can also be formulated by replacing the Young's modulus E and Poisson's ratio μ with $E/(1 + \mu^2)$ and $\mu / (1 - \mu)$ respectively in the stress problem equations. Here, the plane stress elements are used and more details about this class of elements can be found in [19]. We give a brief description of plane stress BSWI_{43} (4 and 3 denote the order m and scale j of the BSWI bases, respectively) elements. The element equilibrium equations can be written as

$$\begin{bmatrix} \mathbf{K}^e_{1,1} & \mathbf{K}^e_{1,2} & \cdots \mathbf{K}^e_{1,n^2+2n} & \mathbf{K}^e_{1,(n+1)^2} \\ \mathbf{K}^e_{2,1} & \mathbf{K}^e_{2,2} & \cdots \mathbf{K}^e_{2,n^2+2n} & \mathbf{K}^e_{2,(n+1)^2} \\ \cdots & \cdots & \cdots & \cdots \\ \mathbf{K}^e_{n^2+2n,1} & \mathbf{K}^e_{n^2+2n,2} & \cdots \mathbf{K}^e_{n^2+2n,n^2+2n} & \mathbf{K}^e_{n^2+2n,(n+1)^2} \\ \mathbf{K}^e_{(n+1)^2,1} & \mathbf{K}^e_{(n+1)^2,2} & \cdots \mathbf{K}^e_{(n+1)^2,n^2+2n} & \mathbf{K}^e_{(n+1)^2,(n+1)^2} \end{bmatrix} \begin{bmatrix} u_1 \\ v_1 \\ \vdots \\ u_{(n+1)^2} \\ v_{(n+1)^2} \end{bmatrix} = \begin{bmatrix} p^e_{a,1} \\ p^e_{b,1} \\ \vdots \\ p^e_{a,(n+1)^2} \\ p^e_{b,(n+1)^2} \end{bmatrix} \tag{3}$$

where $n = 2^j + m - 2 = 2^3 + 4 - 2 = 10$ [19] and the other terms in Eq. (3) are shown as

$$\mathbf{K}^e_{i,j} = \begin{bmatrix} K^{e,1}_{i,j} & K^{e,2}_{i,j} \\ K^{e,3}_{i,j} & K^{e,4}_{i,j} \end{bmatrix} \quad \left(i, j = 1, \cdots, (n+1)^2\right) \tag{4}$$

$$\mathbf{K}^{e,1} = E/(1-\mu^2)\left(\mathbf{A}^{11}_1 \otimes \mathbf{A}^{00}_2 + (1-\mu)/2\,\mathbf{A}^{00}_1 \otimes \mathbf{A}^{11}_2\right) \tag{5}$$

$$\mathbf{K}^{e,2} = E/(1-\mu^2)\left(\mu\mathbf{A}^{10}_1 \otimes \mathbf{A}^{01}_2 + (1-\mu)/2\,\mathbf{A}^{01}_1 \otimes \mathbf{A}^{10}_2\right) \tag{6}$$

$$\mathbf{K}^{e,3} = (\mathbf{K}^{e,2})^{\mathrm{T}} \tag{7}$$

$$\mathbf{K}^{e,4} = E/(1-\mu^2)\left(\mathbf{A}^{00}_1 \otimes \mathbf{A}^{11}_2 + (1-\mu)/2\,\mathbf{A}^{11}_1 \otimes \mathbf{A}^{00}_2\right) \tag{8}$$

$$\begin{aligned}\mathbf{P}^e_a = \left((\mathbf{T}^e_1 \otimes \mathbf{T}^e_1)^{-1}\right)^{\mathrm{T}} \Bigg\{ &\int_{S_\sigma} p_x (\boldsymbol{\Phi}^1)^{\mathrm{T}} \mathrm{d}s + \int_{\Omega_e} f_x (\boldsymbol{\Phi}^1)^{\mathrm{T}} \mathrm{d}\Omega \\ &+ \sum_{i=1}^{n} \left((\mathbf{T}^e_1 \otimes \mathbf{T}^e_1)^{-1}\right)^{\mathrm{T}} \left(\boldsymbol{\Phi}^1(\xi_i, \eta_i)\right)^{\mathrm{T}} F_{ix} \Bigg\}\end{aligned} \tag{9}$$

$$\begin{aligned}\mathbf{P}^e_b = \left((\mathbf{T}^e_1 \otimes \mathbf{T}^e_1)^{-1}\right)^{\mathrm{T}} \Bigg\{ &\int_{S_\sigma} p_y (\boldsymbol{\Phi}^1)^{\mathrm{T}} \mathrm{d}s + \int_{\Omega_e} f_y (\boldsymbol{\Phi}^1)^{\mathrm{T}} \mathrm{d}\Omega \\ &+ \sum_{i=1}^{n} \left((\mathbf{T}^e_1 \otimes \mathbf{T}^e_1)^{-1}\right)^{\mathrm{T}} \left(\boldsymbol{\Phi}^1(\xi_i, \eta_i)\right)^{\mathrm{T}} F_{iy} \Bigg\}\end{aligned} \tag{10}$$

$$\mathbf{A}^{00}_1 = \left((\mathbf{T}^e_1)^{-1}\right)^{\mathrm{T}} \left\{ l_{ex} \int_0^1 (\boldsymbol{\Phi}_3)^{\mathrm{T}} (\boldsymbol{\Phi}_3)\, \mathrm{d}\xi \right\} (\mathbf{T}^e_1)^{-1} \tag{11}$$

$$\mathbf{A}^{01}_1 = \left((\mathbf{T}^e_1)^{-1}\right)^{\mathrm{T}} \left\{ \int_0^1 (\boldsymbol{\Phi}_3)^{\mathrm{T}} \left(\frac{\mathrm{d}\boldsymbol{\Phi}_3}{\mathrm{d}\xi}\right) \mathrm{d}\xi \right\} (\mathbf{T}^e_1)^{-1} \tag{12}$$

$$\mathbf{A}^{10}_1 = (\mathbf{A}^{01}_1)^{\mathrm{T}} \tag{13}$$

$$\mathbf{A}^{11}_1 = \left((\mathbf{T}^e_1)^{-1}\right)^{\mathrm{T}} \left\{ 1/l_{ex} \int_0^1 \left(\frac{\mathrm{d}\boldsymbol{\Phi}_3}{\mathrm{d}\xi}\right)^{\mathrm{T}} \left(\frac{\mathrm{d}\boldsymbol{\Phi}_3}{\mathrm{d}\xi}\right) \mathrm{d}\xi \right\} (\mathbf{T}^e_1)^{-1} \tag{14}$$

The integrals $\mathbf{A}^{ij}_2 (i, j = 0, 1)$ are similar to $\mathbf{A}^{ij}_1 (i, j = 0, 1)$ if element length l_{ex}, differential $\mathrm{d}\xi$ and

https://doi.org/10.1017/jmech.2016.2 Published online by Cambridge University Press

element transfromation matrix $\mathbf{T}_1^e$ are replaced by element width l_{ey}, differential $\mathrm{d}\eta$ and transfromation matrix $\mathbf{T}_2^e$ respectively. It is worth to point out that $K_{i,j}^{e,1}$, $K_{i,j}^{e,2}$, $K_{i,j}^{e,3}$ and $K_{i,j}^{e,4}$ in Eq. (4) are the elements of matrices $\mathbf{K}^{e,1}$, $\mathbf{K}^{e,2}$, $\mathbf{K}^{e,3}$ and $\mathbf{K}^{e,4}$, respectively. $p_{a,1}^e, \cdots, p_{a,(n+1)^2}^e$ and $p_{b,1}^e, \cdots, p_{b,(n+1)^2}^e$ are the elements of column vector $\mathbf{P}_a^e$ and $\mathbf{P}_b^e$, respectively.

In Eqs. (4) ~ (14), f_x and f_y are the components of body forces in the x and y directions, u and v are the components of the displacement vector, p_x and p_y are the components of surface tractions in the x and y directions, respectively; $\mathbf{F}_i = \{F_{xi} \ F_{yi}\}^{\mathrm{T}}$ are point forces and $\mathbf{\Phi}^1(\xi_i, \eta_i)$ are the vectors of the point displacements at the points of application of the point forces.

In this study, the displacement v can be calculated by extrapolation technique as follows [1]

$$v = \frac{K_I}{2G}\sqrt{\frac{r}{2\pi}}(k+1) \tag{15}$$

where r is the distance from crack tip to a point considered along with the crack edge, k is the elastic parameter (For plane stress problem: $k = (3-\mu)/(1+\mu)$, whereas for plane strain problem: $k = 3-4\mu$), G is shear modulus ($G = E/2(1+\mu)$) and K_I is SIFs for mode I.

Therefore, we obtain K_I as

$$K_I = \frac{2Gv}{(k+1)}\sqrt{\frac{2\pi}{r}} \tag{16}$$

3. NUMERICAL INVESTIGATIONS

Example 1. The center crack problem

The central cracked plate and the computational model are in Figs. 1(a) and 1(b) respectively. The plate is subjected to a plane stress condition with symmetrical uniformly distributed load p applied under mode I loading condition. The plate length is $2(b)$, width L and center crack width is $2(a)$.

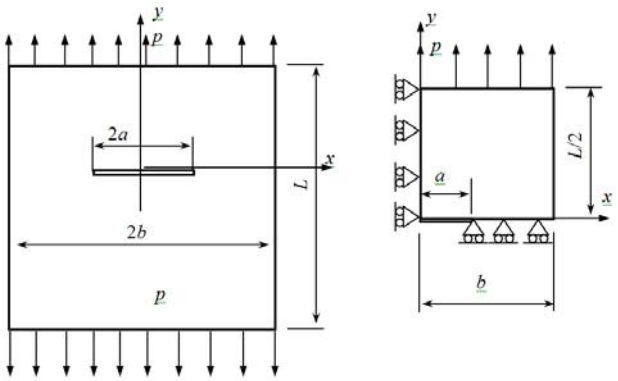
The analytical SIFs for this problem is given in [1] as

$$K_I = p\sqrt{\pi a}F(a/b) \tag{17}$$

To make a simple comparison, the non-dimensional stress intensity factor is defined as follows

$$Z_I = \frac{K_I}{p\sqrt{a}} = \sqrt{\pi}F(a/b) \tag{18}$$

Eight BSWI_{43} elements are employed to calculate this problem. The degrees of freedom (DOFs) of eight BSWI_{43} elements are 1782. In Table 1, the proposed method is compared with the following methods: Method 1: Laurent series solution. The values of $F(a/b)$ are given by Isida [1]. Method 2: Empirical formula. $F(a/b)$ is given by Tada [1], *i.e.*,



(a) The center crack (b) Computational Model

Fig. 1 The center cracked plate and its computational model.

$$F(a/b) = \left\{1 - 0.025\left(\frac{a}{b}\right)^2 + 0.06\left(\frac{a}{b}\right)^4\right\}\sqrt{\sec\frac{\pi a}{2b}} \tag{19}$$

and Method 3: Adaptive finite element method (Traditional plane element are used) with about 5000 DOFs [12].

The present results computed by eight BSWI_{43} elements are found to be in good agreement with those in the literature, as shown in Table 1. When compared with Method 1, the maximum relative error of the proposed method is 1.879% which is lower than that (2.195%) obtained using the adaptive finite element method with about 5000 DOFs, almost three times of that of the 8 BSWL_{43} elements.

Example 2. The double edge crack problem

The double edge cracked plate and its computational model are shown in Figs 2(a) and 2(b) respectively. Like in example 1, we also use only eight BSWI_{43} elements for this problem. To evaluate our method, we compare it with the following two methods in Table 2.

Method 1: Empirical formula. $F(a/b)$ is given by Tada [1]

$$F(a/b) = \frac{1.122 - 0.561\left(\frac{a}{b}\right) - 0.205\left(\frac{a}{b}\right)^2 + 0.471\left(\frac{a}{b}\right)^3 - 0.190\left(\frac{a}{b}\right)^4}{\sqrt{1-\frac{a}{b}}} \tag{20}$$

Method 2: Empirical formula. $F(a/b)$ is given by Benthem [1]

$$F(a/b) = \left(1 + 0.122\cos^4\frac{\pi a}{2b}\right)\sqrt{\frac{2b}{\pi a}\tan\frac{\pi a}{2b}} \tag{21}$$

Method 3: Traditional finite element method (PLANE42 element in software ANSYS) with 200 × 200 meshes (80000 DOFs). PLANE42 is a quadrilateral element that supports a polynomial with an order of one.

https://doi.org/10.1017/jmech.2016.2 Published online by Cambridge University Press

Table 1 Stress intensity factors Z_I for different a/b under uniform tension ($L/2b = 1$) (Example 1).

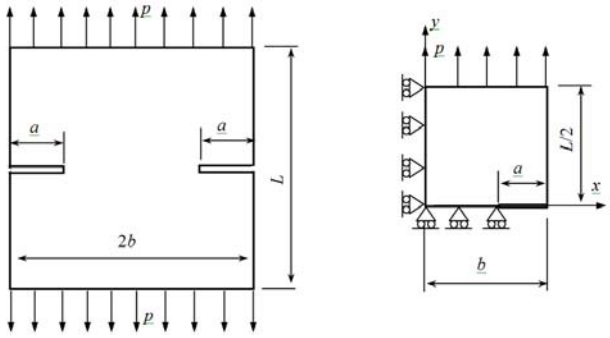
a/b	Method 1		Method 2			Method 3			Proposed method	
	$F(a/b)$	Z_I	$F(a/b)$	Z_I	ε (%)	$F(a/b)$	Z_I	ε(%)	Z_I	ε (%)
0.1	1.006	1.7831	1.006	1.783	0.006	1.001	1.7742	0.499	1.7565	1.492
0.2	1.0246	1.8161	1.0245	1.8158	0.017	1.0237	1.8145	0.088	1.8056	0.578
0.3	1.0557	1.8747	1.0575	1.8744	0.016	1.0416	1.8462	1.520	1.8649	0.523
0.4	1.1094	1.9664	1.109	1.9657	0.036	1.09	1.932	1.749	1.9695	0.158
0.5	1.1867	2.1034	1.1862	2.1025	0.043	1.1879	2.1055	0.100	2.1326	1.388
0.6	1.3033	2.31	1.3028	2.3091	0.039	1.2747	2.2593	2.195	2.3534	1.879
0.7	1.4882	2.6378	1.4874	2.6363	0.057	1.4655	2.5975	1.528	2.6738	1.365
0.8	1.816	3.2188	1.8143	3.2158	0.093	1.8131	3.2136	0.162	3.2563	1.165
0.9	2.5776	4.5687	2.5767	4.567	0.037	2.565	4.5463	0.490	4.5508	0.392

Note: ε in the table denotes the relative error of Z_I obtained using Method 2, Method 3 and the proposed method with respect to that using Method 1.

Table 2 Stress intensity factors Z_I for different a/b under uniform tension ($L/2b = 1$) (Example 2).

a/b	Method 1		Method 2			Method 3		Method 4		Proposed method	
	$F(a/b)$	Z_I	$F(a/b)$	Z_I	ε (%)	Z_I	ε (%)	Z_I	ε (%)	Z_I	ε (%)
0.1	1.1219	1.9885	1.1207	1.9864	0.106	1.8860	5.437	1.9493	1.971	1.9924	0.196
0.2	1.1237	1.9917	1.1185	1.9825	0.462	1.9633	1.446	1.9744	0.869	1.9803	0.572
0.3	1.1312	2.005	1.1198	1.9848	1.007	2.0552	2.443	2.0298	1.237	2.0142	0.459
0.4	1.1491	2.0367	1.1315	2.0056	1.527	2.1471	5.143	2.1341	4.782	2.0830	2.273
0.5	1.1841	2.0987	1.1628	2.061	1.796	2.2309	5.926	2.2032	4.979	2.118	0.920
0.6	1.2471	2.2104	1.2260	2.1731	1.687	2.3181	4.646	2.2389	1.289	2.1999	0.475
0.7	1.3598	2.4102	1.3429	2.3803	1.241	2.4528	1.736	2.4345	1.008	2.4096	0.025
0.8	1.5771	2.7954	1.5667	2.7769	0.662	2.7416	1.961	2.7637	1.134	2.7591	1.299
0.9	2.1179	3.7539	2.1135	3.746	0.210	3.5608	5.424	3.6815	1.929	3.7205	0.890

Note: ε in the table denotes the relative error of Z_I obtained using Method 2, Method 3 and the proposed method with respect to that using Method 1.



(a) The double edge crack (b) Computational Model

Fig. 2 The double-edge cracked plate and its computational model.

Method 4: Traditional finite element method (PLANE145 element in software ANSYS) with 100 × 100 meshes (20000 DOFs).

PLANE145 is a quadrilateral p-element (p is the order of the interpolating polynomial) that supports a polynomial with a maximum order of eight. In the present, $p = 3$ is employed to solve example 2. It notes that the order of the interpolating bases of $BSWI_{43}$ element is also three.

Some computational results are shown in Table 2. As shown in Table 2, by comparing with other methods, the relative errors between results of the proposed method and the empirical formula (Method 1) are less than 2.273% for all a/b values, which are slightly larger than 1.796% of Method 2. Overall, the calculated values are in reasonably good agreement with those obtained by both Method 1 and Method 2. When compared with Method 3, the maximum relative error of the proposed method is much lower than that (5.926%) obtained using the traditional finite element method (PLANE42 element in software ANSYS) with 80000 DOFs, almost forty-five times of that of the 8

https://doi.org/10.1017/jmech.2016.2 Published online by Cambridge University Press

$BSWL_{43}$ elements. Moreover, the relative errors of Method 4 are a little bite larger than those of the present 8 $BSWI_{43}$ elements. However, to obtain the same precision, eleven times of DOFs are needed for the PLANE145 element.

By summarizing the above SIFs analyze and comparisons, the above results of two examples indicate that good calculation accuracy can be achieved for the crack problems by the proposed wavelet-based technique. The main advantage of the proposed method is the time savings due to the substantially reduced number of BSWI elements.

4. CONCLUSIONS

In this paper, the good localization capability of wavelets has been explored to approximate the displacement fields near the crack tip. More specifically, the wavelet-based plane elements using BSWI are employed to simulate singularity problems. The advantage of this method is its computational efficiency. This is reflected by the fact that it requires much less elements, in comparison to the popular finite element method, to achieve the same solution quality. The numerical results show that wavelet finite element method is suitable to compute SIFs for two-dimensional plates.

ACKNOWLEDGEMENTS

The authors are grateful to the support from the National Science Foundation of China (Grant Nos. 51575400, 51505339). This work is also supported in part by the Zhejiang Provincial Natural Science Foundation for Excellent Young Scientists of China (No. LR13E050002), the Zhejiang Technologies R&D Program of China (No. 2014C31103).

REFERENCES

1. Tada, H., Paris, P. C. and Irwin, G. R., *The Stress Analysis of Cracks Handbook*, 3rd Edition, ASME Press, New York, pp. 127–142 (2000).
2. Huang, M. F. and Long, Y. Q., "Calculation of Stress Intensity Factors of Cracked Reissner Plates by the Sub-Region Mixed Finite Element Method," *Computers and Structures*, **30**, pp. 837–840 (1988).
3. Long, Y. and Zhao, Y., "Calculation of Stress Intensity Factors in Plane Problems by the Sub-Region Mixed Finite Element Method," *Advances in Engineering Software*, **7**, pp. 32–35 (1985).
4. Chen, W. H. and Yang, S. H., "Estimation of Stress Intensity Factors in Partially Patched Cracked Composite Laminates by Multilayer Hybrid-Stress Finite Element Method," *Finite Elements in Analysis and Design*, **21**, pp. 21–44 (1995).
5. Miyazaki, N., Ikeda, T., Soda, T. and Munakata, T., "Stress Intensity Factor Analysis of Interface Crack Using Boundary Element Method-Application of Contour-Integral Method," *Engineering Fracture Mechanics*, **45**, pp. 599–610 (1993).
6. Lu, N. C., Cheng, Y. H. and Li, X. G., "Dynamic Problem Concerning Mode I Semi-Infinite Crack Propagation," *Journal of Mechanics*, **29**, pp. 309–317 (2013).
7. Lu, N. C., Li, X. G. and Cheng, Y. H., "Asymmetrical Dynamic Propagation Problem on the Edges of Mode III Interface Crack Subjected to Superimpose Loads," *Journal of Mechanics*, **29**, pp. 318–326 (2013).
8. Chao, C. K. and Wikarta, A., "Anti-Plane Interaction Between a Crack and an Elliptically Cylindrical Layered Media," *Journal of Mechanics*, **29**, pp. 85–93 (2013).
9. Chao, C. K. and Lu, L. M., "Mode-III Stress Intensity Factors of an Arbitrarily Oriented Crack Crossing Interface in a Layered Structure," *Journal of Mechanics*, **29**, pp. 643–651 (2013).
10. Giner, E., Sukumar, N., Tarancón, J. E. and Fuenmayor, F. J., "An Abaqus Implementation of the Extended Finite Element Method," *Engineering Fracture Mechanics*, **76**, pp. 347–368 (2009).
11. Kpegba, K. W. and Ottavy, N., "Stress Intensity Factors in Two-Dimensional Crack Problems by Using the Superimposed Meshes Method," *Engineering Fracture Mechanics*, **54**, pp. 113–125 (1996).
12. Souiyah, M., Alshoaibi, A., Muchtar, A. and Ariffin, A. K., "Two-Dimensional Finite Element Method for Stress Intensity Factor Using Adaptive Mesh Strategy," *Acta Mechanics*, **204**, pp. 99–108 (2009).
13. Yang, X. Q., "A Special Crack Tip Displacement Discontinuity Element," *Mechanics Research Communication*, **31**, pp. 651–659 (2004).
14. Meshii, T. and Watanabe, K., "Stress Intensity Factor Error Index for Finite Element Analysis with Singular Elements," *Engineering Fracture Mechanics*, **70**, pp. 657–669 (2003).
15. Daimon, R. and Okada, H., "Mixed-Mode Stress Intensity Factor Evaluation by Interaction Integral Method for Quadratic Tetrahedral Finite Element with Correction Terms," *Engineering Fracture Mechanics*, **115**, pp. 22–42 (2014).
16. Chiang, C. H. and Cheng, C. C., "Detecting Rebars and Tubes Inside Concrete Slabs Using Continuous Wavelet Transform of Elastic Waves," *Journal of Mechanics*, **20**, pp. 297–302 (2004).
17. Yang, T. S., Shy, S. S. and Chyou, Y. P., "Spatio-temporal Intermittency Measurements in a Gas-Phase Near-Isotropic Turbulence Using High-Speed DPIV and Wavelet Analysis," *Journal of Mechanics*, **21**, pp. 157–169 (2005).
18. Canuto, C., Tabacco, A. and Urban, K., "The Wave-

https://doi.org/10.1017/jmech.2016.2 Published online by Cambridge University Press

let Element Method Part II: Realization and Additional Feature in 2D and 3D," *Applied and Computational Harmonic Analysis*, **8**, pp. 123–165 (2000).

19. Xiang, J. W., Chen, X. F., He, Y. M. and He, Z. J., "The Construction of Plane Elastomechanics and Mindlin Plate Elements of B-Spline Wavelet on the Interval," *Finite Elements in Analysis and Design*, **42**, pp. 1269–1280 (2006).
20. Xiang, J. W., Chen, X. F., He, Z. J. and Zhang, Y. H., "A New Wavelet-Based Thin Plate Element Using B-Spline Wavelet on the Interval," *Computational Mechanics*, **41**, pp. 243–255 (2008).
21. Zhang, X. W., Chen, X. F. and Wang, X. Z., "Multivariable Finite Elements Based on B-Spline Wavelet on the Interval for Thin Plate Static and Vibration Analysis," *Finite Elements in Analysis and Design*, **46**, pp. 416–427 (2010).
22. Zhang, X. W., Chen, X. F. and Yang, Z. B., "Multivariable Wavelet Finite Element for Flexible Skew Thin Plate Analysis," *Science in China Technology Science*, **57**, pp. 1532–1540 (2014).
23. Yang, Z. B., Chen, X. F. and Zhang, X. W., "Free Vibration and Buckling Analysis of Plates Using B-Spline Wavelet on the Interval Mindlin Element," *Applied Mathematical Modeling*, **37**, pp. 3449–3466 (2013).
24. Cohen, A., *Numerical Analysis of Wavelet Method*, Elsevier Press, Amsterdam, pp. 32–35 (2003).
25. Li, B. and Chen, X. F., "Wavelet-Based Numerical Analysis: A Review and Classification," *Finite Elements in Analysis and Design*, **81**, pp. 14–31 (2014).
26. Chui, C. K. and Quak, E., "Wavelets on a Bounded Interval," *Numerical Methods in Approximation Theory*, **9**, pp. 53–77 (1992).
27. Mallat, S., *A Wavelet Tour of Signal Processing*, Academic Press, London, pp. 1–34 (1999).

(Manuscript received October 31, 2014, accepted for publication October 30, 2015.)

https://doi.org/10.1017/jmech.2016.2 Published online by Cambridge University Press